

7. MEASUREMENT OF INTENSITIES

Compton profile – the projection of the electron momentum density distribution onto the X-ray scattering vector – can be isolated from the relativistic differential scattering cross section within the impulse approximation. Several experimental and theoretical investigations have been concerned with understanding the changes in the spectral distribution when electron binding energies cannot be discounted. It has been found (*e.g.* Pattison & Schneider, 1979; Bloch & Mendelsohn, 1974) that, to a high degree of accuracy, the spectral distribution is merely truncated at energy transfers $E \leq E_B$.

This has led to the suggestion that the incoherent intensity can be obtained by integrating the spectral distributions, *i.e.* from

$$\frac{d\sigma}{d\Omega} = \int_{E_1 - E_B}^{\infty} \frac{d^2\sigma}{d\Omega dE_2} dE_2. \quad (7.4.3.6)$$

Unfortunately, this requires the Compton profile of each electron shell as input [Compton line shapes have been tabulated by Biggs, Mendelsohn & Mann (1975)] for all elements.

Ribberfors (1983) and Ribberfors & Berggren (1982) have shown that this calculation can be dramatically simplified, without loss of accuracy, by crudely approximating the Compton line shape. Fig. 7.4.3.2 shows the incoherent scattering from aluminium, modelled in this way, and compared with experiment, Waller–Hartree theory, and an exact integral of the truncated impulse Compton profile.

7.4.3.4. Plasmon, Raman, and resonant Raman scattering

In typical X-ray experiments, as is evident from Table 7.4.3.1, the energy transfer may be so low that Compton scattering will be inhibited from all but the most loosely bound electrons. Indeed, in the situation in metals where \mathbf{K} , the momentum transfer, is less than \mathbf{k}_F (the Fermi momentum), Compton scattering from the conduction electrons may be restricted by exclusion because of the lack of unoccupied final states [see Bushuev & Kuz'min (1977)].

Fortunately, in these uncertain circumstances, the incoherent intensities are low. In this regime, the electron gas may be excited into collective motion. For almost all solids, the plasmon excitation energy is 20–30 eV and, in the random phase approximation, the incoherent scattering factor becomes $S(\Delta E, \mathbf{K}) \propto (K^2/w_p)\delta(\Delta E - h\omega_p)$, where ω_p is the plasma frequency.

At slightly higher energies ($\Delta E \geq E_B$), Compton scattering and Raman scattering can coexist, though the Raman component is only evident at low momentum transfer (Bushuev & Kuz'min, 1977). The resultant spectrum is often referred to as the Compton–Raman band. In semi-classical radiation theory, Raman scattering is usually differentiated from Compton scattering by dropping the requirement for momentum conservation between the photon and the individual target electron, the recoil being absorbed by the atom. The Raman band corresponds to transitions into the lowest unoccupied levels and these can be calculated within the dipole approximation as long as $|\mathbf{K}|a < 1$, where \mathbf{K} is the momentum transfer and a the orbital radius of the core electron undergoing the transition. The transition probability in equation (7.4.3.4) becomes

$$\sum_f |\langle \psi_f | \mathbf{r} | \psi_i \rangle|^2 \delta(E_f - E_i - \Delta E), \quad (7.4.3.7)$$

which implies that the near-edge structure is similar to the photoelectric absorption spectrum.

Whereas plasmon and Raman scattering are unlikely to make dramatic contributions to the total incoherent intensity, resonant Raman scattering (RRS) may, when $E_1 \leq E_B$. The excitation involves a virtual *K*-shell vacancy in the intermediate state and a vacancy in the *L* (or *M* or *N*) shell and an electron in the continuum in the final state. It has now been observed in a variety of materials [see, for example, Sparks (1974), Eisenberger, Platzman & Winick (1976), Schaupp *et al.* (1984)]. It was predicted by Gavrilu & Tugulea (1975) and the theory has been treated comprehensively by Åberg & Tulkki (1985). The effect is the exact counterpart, in the inelastic spectrum, of anomalous

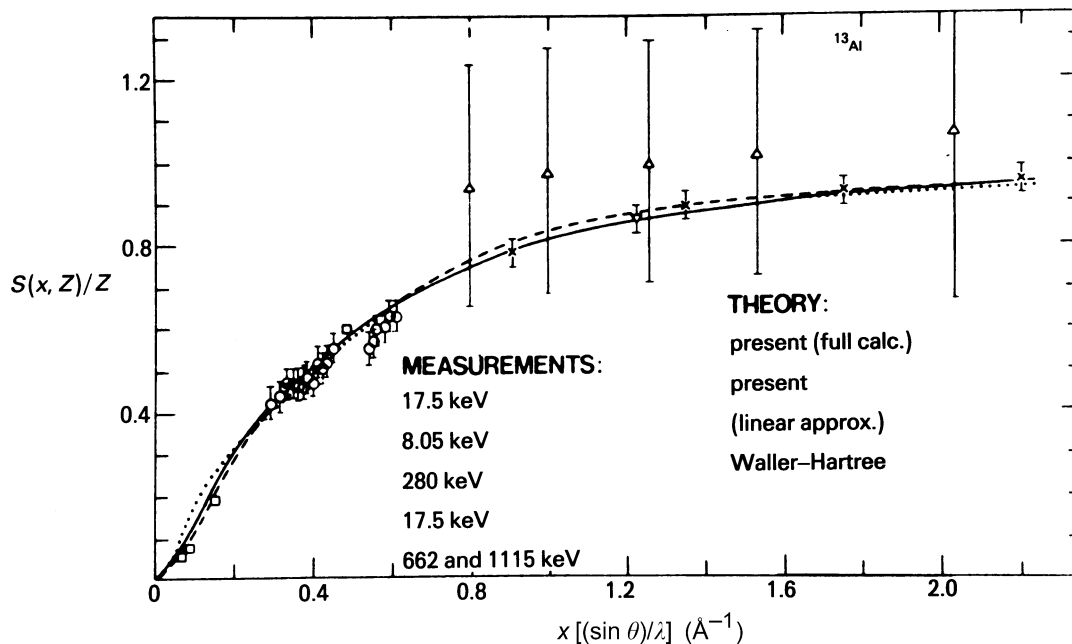


Fig. 7.4.3.2. The incoherent scattering function, $S(x, Z)/Z$, per electron for aluminium shown as a function of $x = (\sin \theta)/\lambda$. The Waller–Hartree theory (\cdots) is compared with the truncated impulse approximation in the tabulated Compton profiles (Biggs, Mendelsohn & Mann, 1975) cut-off at $E < E_B$ for each electron group (---). The third curve (---) shows the simplification introduced by Ribberfors (1983) and Ribberfors & Berggren (1982). The predictions are indistinguishable to within experimental error except at low $(\sin \theta)/\lambda$. Reference to the measurements can be found in Ribberfors & Berggren (1982).